Simulation of high energy photoelectron diffraction using many-beam dynamical Kikuchi-band theory

Aimo Winkelmann,* Bernd Schröter, and Wolfgang Richter
Institut für Festkörperphysik, Friedrich-Schiller-Universität, Max-Wien-Platz 1, D-07743 Jena, Germany

We use the many-beam dynamical theory of electron diffraction for the calculation of x-ray photoelectron diffraction (XPD) patterns of the substrate emission. The reciprocity principle is used to apply a Bloch wave model for the diffraction of an incoming plane wave by a three-dimensional crystal. In this way, many-beam dynamical simulations of XPD in the context of Kikuchi-band theory can be carried out. This extends the results of the two-beam theory used so far and leads to quantitative descriptions of XPD patterns in the picture of photoelectrons reflected by lattice planes. The effects of forward scattering directions, substrate polarity, circular structures due to onedimensional diffraction, and emitter specific extinction of Kikuchi lines can be reproduced by Kikuchi-band theory. The results are compared with single scattering cluster calculations. In this way, the equivalence of the cluster approach and the Kikuchi-band picture can be demonstrated completely in both directions

I. INTRODUCTION

The method of x-ray photoelectron diffraction (XPD) is a powerful tool for the analysis of crystal surfaces and adsorbates. By measuring the angular intensity of photoelectrons excited by x rays and comparing the experimental data with simulations, information on the surface crystallography of the investigated sample can be gained.[1]

Early observations on single crystal surfaces have interpreted the angular distributions as caused by reflection of the photoelectrons on lattice planes of the three-dimensionally periodic bulk crystal.[2] This is a special case of emission from point sources inside a crystal for which a general description was given using dynamical many-beam theory applying a plane wave expansion of the diffracted electron waves.[3,4] A two-beam dynamical theory was applied to explain the azimuthal variations of photoelectron intensities for single crystal copper.[5] Using this theory, the intensity variations could be reproduced by the summation of a number of so-called Kikuchi bands. These bands show increased intensity in a region of a width which is twice the Bragg angle of the corresponding reflecting lattice plane.

Photoelectrons with low kinetic energies of typically less than 2 keV, however, only sample a finite depth which can be as small as a few atomic layers. On these length scales, the properties of the surface become important and photoelectron diffraction has to be described by a theory which can handle the possible loss of symmetry.

If long-range order is still present, layer-by-layer methods can make efficient use of the two-dimensional translation symmetry of surfaces. These methods apply theoretical principles which originated in the context of low-energy electron diffraction (LEED)[6–9] and reflection high-energy diffraction (RHEED).[10]

One of the most successful computational schemes is the cluster approach which allows the description of almost arbitrary surface structures in a very natural way. This is made possible by the short inelastic mean free path of the photoelectrons. Only a limited number of scatterers in the neighborhood of an emitter contribute to the diffraction process, which can thus be effectively handled in a real-space formulation of the theory with no further assumptions about symmetries. Cluster calculations have been used in a number of experimental investigations, applying single and multiple scattering.[11–16] Fast calculations are possible based on certain approximations for spherical wave scattering in photoelectron diffraction, especially the separable-propagator method of Rehr and Albers,[17] the concentric-shell algorithm of Saldin *et al.*[18] and the reduced angular momentum expansion of Fritzsche *et al.*[19]

Cluster simulations were successful in reproducing the formation of Kikuchi bands in substrate XPD measured with high resolution.[20,21] It was shown that these bands become more pronounced the larger the number of scatterers in a cluster is. This is the case at the high-energy end of the XPD method with photoelectron kinetic energies of 1 to 2 keV. Especially in light elements and compounds, the clusters needed at these energies can contain several thousand atoms in accordance with the inelastic mean free path. This makes multiple scattering cluster calculations very time and memory consuming.

With increasing cluster sizes, the surface properties should become less and less important, leading to enhanced bulk characteristics in the diffraction pattern. Therefore it should also be possible to simulate these high-energy substrate XPD patterns using many-beam dynamical Kikuchi-band (or electron channeling) theory. These many-beam calculations are made possible by the increase in computer speed and memory which allows a large number of reflecting planes to be taken into account simultaneously. Returning to the earliest interpretation of substrate XPD patterns, we will show that this theory can not only explain the formation of Kikuchi bands but also reproduces features such as forward-

scattering directions and ring-shaped interference maxima around these directions. Such features can also be explained in the intuitive forward scattering picture of cluster calculations. The advantage of Kikuchi-band theory for substrate XPD lies in the fact that the Kikuchi lines are already part of the theory and do not emerge as a secondary phenomenon from a huge number of periodically arranged scatterers.

Comparing dynamical theory with single scattering cluster calculation we provide a "translation" between terms used in high-energy electron diffraction theory—which operates in reciprocal space—and the real-space cluster theory. In this way we show that the electron channeling picture of Kikuchi-band theory is a valid description of the substrate photoelectron diffraction process at high energies, a view which was previously in question.[22]

II. THEORY

For the description of the photoelectron diffraction process by a channeling picture we assume that the electrons originate isotropically from point sources which are periodically arranged inside a crystal. The outgoing photoelectrons are scattered by the crystal and detected as a plane wave at the detector. By using reciprocity principle one realizes that this is equivalent to the problem of an incoming electron beam which is diffracted by the crystal and were the electron intensity at the emitting atoms is sought.[3,4]

The diffraction of a parallel electron beam impinging on a sample is of importance in various methods of electron microscopy. From a principal point of view, the atom location by channeling-enhanced microanalysis (ALCHEMI) technique[23] is closely related to the problem of substrate XPD. In ALCHEMI, an incoming electron beam excites characteristic x rays dependent on its tilt relative to the crystal. If the diffraction of the incoming beam concentrates a larger amount of electrons near atoms, increased ionization and therefore also increased x-ray fluorescence will result. Reversing the direction from the ionization process to an outgoing plane wave, one practically looks at the method of XPD. This is why ALCHEMI-type of experiments have also been termed "inverted XPD".[24]

The close analogy to incoming-beam channeling effects allowed us to use existing algorithms for the application to substrate XPD. A Bloch wave approach is used to describe the diffraction of incoming electrons with wave vector $\mathbf{k}_0$. The use of this method is described in several reviews.[25,26] In the following, we give a short summary of the basic theory we applied.

The wave function inside the crystal is described as a superposition of Bloch waves with wave vectors $\mathbf{k}^{(j)}$

$$\Psi(\mathbf{r}) = \sum_j c_j \exp(i\mathbf{k}^{(j)} \cdot \mathbf{r}) \sum_g C_g^{(j)} \exp(i\mathbf{g} \cdot \mathbf{r}). \quad (1)$$

One introduces the total (scaled) potential $U(\mathbf{r})$:

$$U(\mathbf{r}) = U^c(\mathbf{r}) + iU'(\mathbf{r}) = \sum_{\mathbf{g}} U_{\mathbf{g}} \exp(i\mathbf{g} \cdot \mathbf{r}). \quad (2)$$

The potential is described by complex electron structure factors $U_g^c = 2mV_{\mathbf{g}}/\hbar^2$ with $V_{\mathbf{g}}$ being a Fourier coefficient of the crystal potential in eV and the relativistic electron mass m. Inelastic effects are included by the definition of the imaginary components $U'_{\mathbf{g}}$.

Substitution of these expressions for the wavefunction and the potential into the Schrödinger equation leads to the standard dispersion relation

$$[\mathbf{K}^2 - (\mathbf{k}^{(j)} + \mathbf{g})^2]C_{\mathbf{g}}^{(j)} + \sum_h U_{\mathbf{g-h}}C_{\mathbf{h}}^{(j)} = 0. \quad (3)$$

$\mathbf{K}$ is the electron wave vector inside the crystal, $k_0^2 = K^2 - U_0^c$. Then $\mathbf{k}^{(j)}$ is written as

$$\mathbf{k}^{(j)} = \mathbf{K} + \lambda^{(j)}\mathbf{n}, \quad (4)$$

where $\mathbf{n}$ is a unit vector normal to the surface to transform Eq. (3) into an eigenvalue problem[26] which gives the eigenvalues $\lambda^{(j)}$ and eigenvectors with elements $C_{\mathbf{g}}^{(j)}$. This includes effects due to the tilt of the outgoing direction up to about 80° relative to the surface[27] and is valid for arbitrary reciprocal space vectors $\mathbf{g}$. Only Bloch waves which travel outwards in direction to the surface are considered in the case of XPD, backscattered waves are neglected in this approach.

The boundary conditions at the surface determine the coefficients c_j in Eq. (1). These quantities are given by the elements of the first column of the inverse of the matrix whose elements are $C_{\mathbf{g}}^{(j)}$.[26] After this, the wave function (1) is known and can be used to calculate the electron probability density inside the crystal. The wave function is known at all emitter sites after a single calculation. This is an advantage of the path-reversed approach[7] for the simulations of the substrate emission. In cluster calculations, a separate computation has to be carried out for each emitter.

Isotropic absorption corresponds to an inelastic mean free path Λ_e of the electrons and is described by the constant part V'_0 (in eV) of the imaginary part of the total potential[5]

$$V'_0 = -(\hbar^2 E/2m)^{1/2}\Lambda_e. \quad (5)$$

Spatially nonisotropic absorption effects (corresponding to coefficients $V'_{\mathbf{g}}$ with $\mathbf{g} \neq 0$) were not considered[5] for the simulations to be comparable to the cluster calculations where isotropic absorption corresponding to an inelastic mean free path is usually assumed. The Fourier coefficients $V_{\mathbf{g}}$ of the real part of the crystal potential can be calculated from the contributions of the atoms which constitute the unit cell

$$V_{\mathbf{g}} = \frac{1}{\Omega} \sum_i f^e(s) \exp(-i\mathbf{g} \cdot \mathbf{r}_i) \quad (6)$$

with the atoms at positions $\mathbf{r}_i$ in the unit cell volume Ω and the Fourier coefficients $f^e(s)$, $s = |\mathbf{g}|/2$ of the atomic potentials. The $f^e(s)$ are calculated from parameters tabulated in the literature by Doyle and Turner.[28]

To compute the probability of electrons to be at the atomic sites of the emitters one has to calculate $\psi\psi^*$ from Eq. (1).[27] The interaction of diffracted electrons with the crystal atoms has been modeled by generalized potentials.[29,30] In the case that these potentials have the form of delta functions
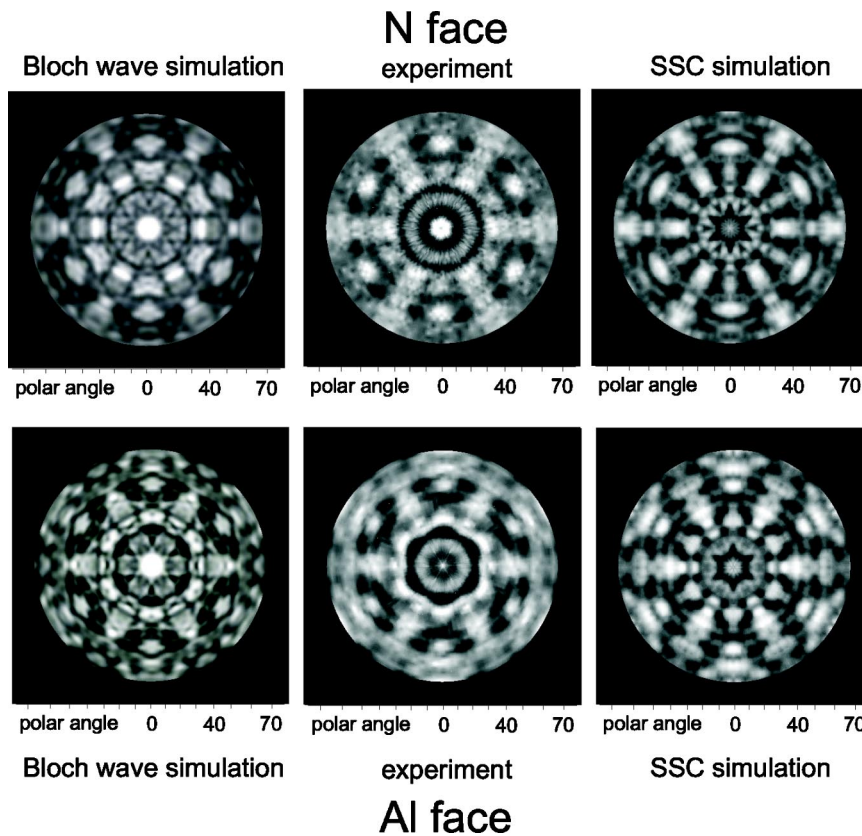
FIG. 1. XPD patterns of AlN{0001}, Al2p, $E_{\mathrm{kin}}=1413$ eV.

(point sources) which are broadened by thermal vibrations, Rossouw et al.[31] have given the following expression for the depth integrated intensity at the crystal atoms:

$$I \propto \sum_{n,ij} B^{ij}(t) \sum_{\mathbf{g},\mathbf{h}} C_{\mathbf{g}}^{(i)} C_{\mathbf{h}}^{(j)*} \exp(-M_{\mathbf{g-h}}^{n}) \exp[i(\mathbf{g-h}) \cdot \mathbf{r}_n]$$

$$(7)$$

with atoms at $\mathbf{r}_n$, Debye-Waller factors $\exp(-M_{\mathbf{g-h}}^n)$ and a depth integrated interference term $B^{ij}(t)$ of the Bloch waves i and j:

$$B^{ij}(t) = c_i c_j \frac{\exp[i(\lambda^i - \lambda^{j*})t] - 1}{i(\lambda^i - \lambda^{j*})}.$$

$$(8)$$

For the calculation of the Bloch waves, we have applied a program published by Zuo et al.[26,32] We modified this code to include the channeling effects according to the approach outlined above. The Debye-Waller factors we took from a parametrization of Gao et al.[33]

Our assumption of simple isotropical photoelectron emission compared to a more correct description of the ionization process is made because of simplicity to gain insight into the fundamental processes of channeling in photoelectron diffraction. Matrix-element effects of the $l \pm 1$ channels at the ionization could be incorporated into the theory in principle by the use of generalized potentials.[29,30] Due to the strong forward scattering, the influence of these effects should be reduced at high kinetic energies.

The assumption of a threedimensionally periodic crystal and the neglect of backscattered waves indicate that the approach described here is only valid at the high energy end of the XPD technique. Effects such as surface reconstructions and surface relaxation as well as increased backscattering become significant at low energies. These effects are handled very effectively by the various methods mentioned above. The approach described here is clearly focussed on the single crystal substrate emission at relatively high kinetic energies.

For the comparison of the channeling simulations with cluster calculations, we have used a single scattering cluster model described elsewhere.[34] It has been shown that clusters with up to ten emitter layers and up to 20 Å in radius are necessary for correct simulations of substrate XPD.[34]

III. RESULTS

A. Polarity of aluminium nitride {0001}

The determination of the polarity of noncentrosymmetric crystals is a problem which cannot be solved by two-beam channeling theory alone. This is why we use this problem as a first example for the applicability of the dynamical theory. We have shown previously that SSC calculations can reproduce the differences in the XPD patterns of surfaces of different polarity.[34] In Fig. 1 we show the Al2p patterns of the (0001) and $(000\bar{1})$ faces of aluminum nitride (AlN). The Al2p electrons were excited by AlK$_\alpha$ radiation. Full experimental details are given elsewhere.[35]
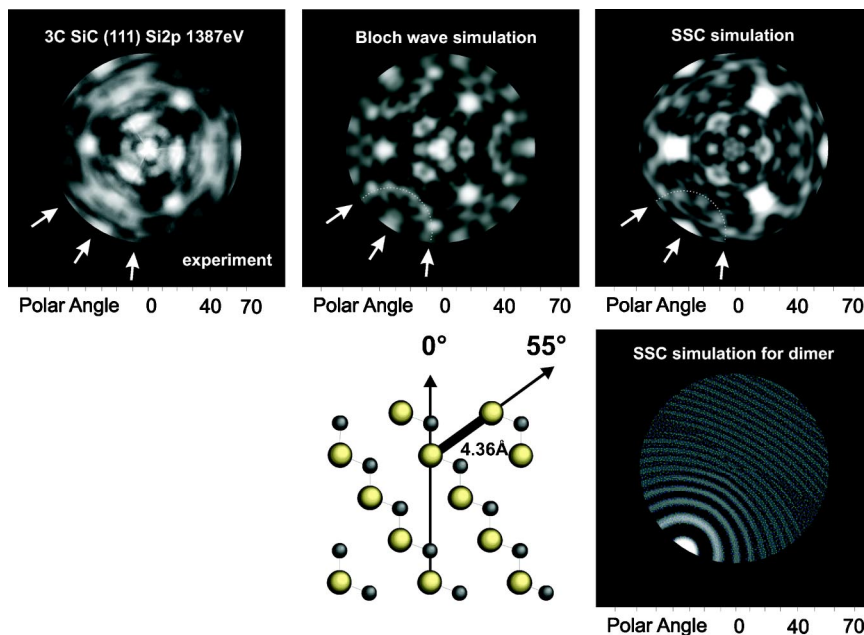
FIG. 2. Experimental and simulated XPD patterns of 3C SiC(111), Si2p, E_{kin} = 1387 eV.

From the dynamical theory it can be deduced that there should be an asymmetry between the reflections on either side of a lattice plane. This leads to differences in the shape of Kikuchi bands from samples of different polarity.[27,36] For the dynamical simulations, 238 reflecting planes with a minimum spacing d_{hkl} of 0.9 Å have been used. The calculated patterns were drawn in stereographic projection and smoothed according to the angular resolution of the detector of about 2°.

There is a clear difference in the measured patterns of the Al and the N faces. Comparison with the simulated data shows good agreement in the structures which are seen in the hemispherical diffraction patterns for both the SSC and the Bloch wave simulations. Limitations are found in the reproduction of the relative intensities and the structures in normal emission. For the SSC calculations this can be attributed to multiple scattering effects.[34]

This shows that the dynamical theory can reproduce the changes in the diffraction patterns from surfaces of different polarity. In the single scattering picture this can be explained by the different scattering strengths of the aluminium and nitride atoms which reside near the surface.[35]

B. Reciprocal vs real space interpretation

Comparing the intuitive forward scattering interpretation of the cluster picture with the reciprocal space channeling theory one can ask if it is possible to relate different parts of these theories to each other. In Fig. 2 we show the Si2p XPD pattern of cubic silicon carbide (3C SiC). The threefold pattern is dominated by three strong forward scattering maxima at 35° polar angle. In addition, one finds ringlike structures around the directions at 55° polar angle. These structures can be explained by the directions of nearest silicon atoms in the SiC crystal structure. The corresponding SSC calculation shows a good agreement between theory and experiment,

except for the fact that the strongest maxima are too broad. This is a well known property of single scattering calculations.

The measured pattern does not give a typical Kikuchi-band impression, which is partly due to the angular resolution of about 2°. Nonetheless, the corresponding Bloch wave simulation using 280 reflecting planes after accounting for the limited detector resolution shows a very good agreement with the experiment. The relative intensities are reproduced better than in the SSC simulations.

At first sight, it seems astonishing that the Kikuchi-band picture is able to explain the ringlike structures in the diffraction pattern. One such ring is marked in Fig. 2 around the [010] direction. In the forward scattering picture, this ring can be interpreted as the first order maximum of the diffraction taking place at the emitter-scatterer pair which is shown in Fig. 2.

The opening angle 2θ of these rings is determined by the distance r, the wave number k of the electron and the scattering phase shift $\Delta\phi$:[37]

$$kr(1 - \cos 2\theta) + \Delta\phi(2\theta) = 2\pi. \qquad (9)$$

By measuring the opening angle of the ring, the emitter-scatterer distance can be inferred. In Fig. 2, there is also shown a SSC simulation of the emitter-scatterer pair with a distance of 4.36 Å. This simulation very nicely shows the zeroth order forward scattering maximum and the ring-shaped first order maximum.

The Bloch wave simulation in Fig. 2 also shows the maximum and the ring at about 55° polar angle. This ring is the envelope of a number of reflecting planes. These reflexes are strongly excited when the Ewald sphere cuts reciprocal space points which do not lie at right angles to the zone axis. This is shown in Fig. 3. The corresponding rings are called "first order Laue zone" (FOLZ) rings.[26]
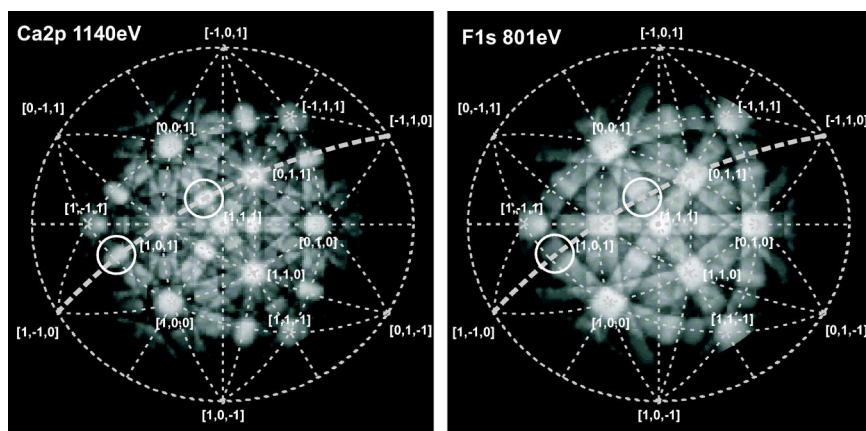
FIG. 3. Simulated XPD patterns of Ca2p (1140 eV) and F1s (801 eV) from CaF$_2$(111), 63 reflecting planes.

Both the reciprocal space picture with reflecting lattice planes and the real space cluster picture allow the determination of crystal lattice parameters from the opening half angle 2θ of the rings.[37,38] For simplicity we look at a lattice with atoms placed in such a way that the distance H (in Å) between the atoms corresponds to the reciprocal lattice plane spacing H^{-1} in Å^{-1} (Fig. 3). Also, the scattering factors are assumed to be real according to the Born approximation, which is valid at high energies.

From Fig. 3(a) one sees that $H^{-1}=K-K\cos 2\theta$, with the inverse of the electron wavelength K. In real space one has to look at the path length differences between the scattering at the first and the second atom and set this difference equal to the electron wavelength for the first order maximum. This requires that $H-H\cos 2\theta=\lambda=K^{-1}$ which is seen from Fig. 3(b) and gives the same H as in reciprocal space. This shows that at high energies, the ring like structures can be equally interpreted as FOLZ rings (in the language of high energy electron diffraction) as well as first order interference maxima along forward scattering directions (in the language of cluster photoelectron diffraction).

C. Site specific extinction of Kikuchi lines

Element specific extinctions of Kikuchi lines have been observed by Omori *et al.*[39,40] and explained using two-beam dynamical theory. The effects have been reproduced by multiple scattering cluster calculations.[20] We use this example to
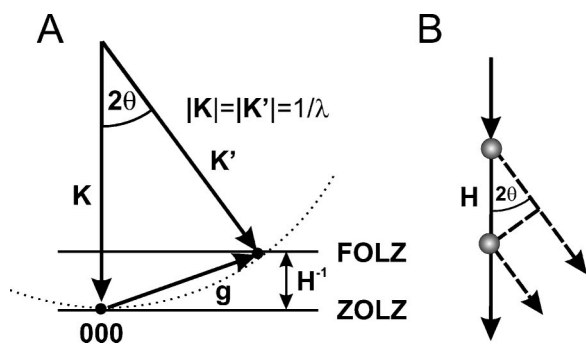
show how a very effective interpretation is possible using Kikuchi-band theory.

In Fig. 4 we show the simulated XPD patterns of the Ca2p and F1s electrons of CaF$_2$(111). A set of 63 reflecting planes was selected to match those seen in the experimental data of Omori *et al.*[40] Comparing both patterns, the Kikuchi lines in the F1s pattern are broadened due to the smaller energy of the photoelectrons. Also, the three $\{\bar{1}11\}$ reflections are missing in the F1s pattern. To explain this behavior, an element specific extinction rule was applied.[40] This rule implies that the extinction of element-specific Kikuchi-bands depends on a combination of the lattice site of the source atoms and the structure factor. The $(11\bar{1})$ reflection is marked bold in Fig. 4. The effects of the extinction of this band reach over the whole area of the diffraction pattern. For comparison, two regions of interest in the figure are marked with circles. In the cluster picture, one would have to discuss several existing or missing forward scattering and interference directions to explain the intensity enhancement or decrease. The Kikuchi-band picture allows one to name a specific reflecting plane as the cause for both features (and all other features related to this plane). The simulated patterns of Fig. 4 complement the cluster simulations of Bardi *et al.*[20] who demonstrated the formation of Kikuchi bands with large clusters.

IV. SUMMARY

We applied a many-beam dynamical theory of electron diffraction to the problem of the calculation of x-ray photoelectron diffraction patterns of the substrate emission. Many-beam dynamical simulations of XPD in the context of Kikuchi-band theory have been carried out for AlN, SiC, and CaF$_2$. These simulations extend the results of the two-beam theory used so far and lead to quantitative descriptions of XPD patterns in the picture of photoelectrons reflected by lattice planes. The effects of forward scattering directions, substrate polarity, circular structures due to onedimensional diffraction and emitter specific extinction of Kikuchi lines can be reproduced by Kikuchi-band theory. The results have been compared with single scattering cluster calculations. In this way, the equivalence of the cluster approach and the Kikuchi-band picture can be shown in both directions, which was not explicitly done so far.

FIG. 4. Conditions for the formation of ringlike structures in reciprocal (a) and real space (b).

*Electronic address: aimo.winkelmann@epost.de

[1] C. S. Fadley, in *Synchrotron Radiation Research: Advances in Surface Science*, edited by R. Z. Bachrach (Plenum Press, New York, 1992), Vol. 2, pp. 421–518.

[2] K. Siegbahn, U. Gelius, H. Siegbahn, and E. Olson, Phys. Scr. **1**, 272 (1970).

[3] M. von Laue, *Materiewellen und ihre Interferenzen* (Akademische Verlagsgesellschaft Geest & Portig, Leipzig, 1948).

[4] R. E. DeWames and W. F. Hall, Acta Crystallogr., Sect. A: Cryst. Phys., Diffr., Theor. Gen. Crystallogr. **24**, 206 (1968).

[5] S. M. Goldberg, R. J. Baird, S. Kono, N. F. T. Hall, and C. S. Fadley, J. Electron. J. Electron Spectrosc. Relat. Phenom. **21**, 1 (1980).

[6] J. B. Pendry, *Low Energy Electron Diffraction* (Academic Press, London and New York, 1974).

[7] M. D. Pauli and D. K. Saldin, Phys. Rev. B **64**, 075411 (2001).

[8] J. B. Pendry, Surf. Sci. **57**, 679 (1976).

[9] C. H. Li and S. Y. Tong, Phys. Rev. Lett. **42**, 901 (1979).

[10] J. F. Hart and J. L. Beeby, Surf. Sci. **424**, 94 (1999).

[11] S. Kono, S. M. Goldberg, N. F. T. Hall, and C. S. Fadley, Phys. Rev. B **22**, 6085 (1980).

[12] K.-M. Schindler, V. Fritzsche, M. C. Asensio, P. Gardner, D. E. Ricken, A. W. Robinson, A. M. Bradshaw, D. P. Woodruff, J. C. Conesa, and A. R. González-Elipe, Phys. Rev. B **46**, 4836 (1992).

[13] J. Osterwalder, P. Aebi, R. Fasel, D. Naumovic, P. Schwaller, T. Kreutz, L. Schlapbach, T. Abukawa, and S. Kono, Surf. Sci. **331-333**, 1002 (1995).

[14] P. Schieffer, G. Jezequel, B. Lepine, D. Sebilleau, G. Feuillet, and B. Daudin, Surf. Sci. **482-485**, 593 (2001).

[15] J. Hayoz, T. Pillo, R. Fasel, L. Schlapbach, and P. Aebi, Phys. Rev. B **59**, 15 975 (1999).

[16] P. J. Hardman, P. Wincott, G. Thornton, A. Kaduwela, and C. S. Fadley, Phys. Rev. B **60**, 11 700 (1999).

[17] Y. Chen, F. J. G. de Abajo, A. Chassé, R. X. Ynzunza, A. P. Kaduwela, M. Van Hove, and C. S. Fadley, Phys. Rev. B **58**, 13 121 (1998).

[18] D. K. Saldin, G. R. Harp, and X. Chen, Phys. Rev. B **48**, 8234 (1993).

[19] V. Fritzsche and P. Rennert, Phys. Status Solidi B **135**, 49 (1986).

[20] U. Bardi, M. Torrini, Y. Ichinoe, S. Omori, H. Ishii, M. Owari, and Y. Nihei, Surf. Sci. **394**, L150 (1997).

[21] O. M. Küttel, R. G. Agostino, R. Fasel, J. Osterwalder, and L. Schlapbach, Surf. Sci. **312**, 131 (1994).

[22] W. F. Egelhoff, Phys. Rev. Lett. **59**, 559 (1987).

[23] J. C. H. Spence and J. Tafto, J. Microsc. **130**, 147 (1983).

[24] S. Evans, J. Phys.: Condens. Matter **9**, 1967 (1997).

[25] C. J. Humphreys, Rep. Prog. Phys. **42**, 1825 (1979).

[26] J. C. H. Spence and J. M. Zuo, *Electron Microdiffraction* (Plenum Press, New York, 1992).

[27] L. J. Allen and C. J. Rossouw, Phys. Rev. B **39**, 8313 (1989).

[28] P. A. Doyle and P. S. Turner, Acta Crystallogr., Sect. A: Cryst. Phys., Diffr., Theor. Gen. Crystallogr. **24**, 390 (1968).

[29] L. J. Allen and C. J. Rossouw, Phys. Rev. B **42**, 11 644 (1990).

[30] L. J. Allen and C. J. Rossouw, Phys. Rev. B **47**, 2446 (1993).

[31] C. J. Rossouw, P. R. Miller, T. W. Josefsson, and L. J. Allen, Philos. Mag. A **70**, 985 (1994).

[32] J. M. Zuo, K. Gjonnes, and J. C. H. Spence, J. Electron Microsc. Tech. **12**, 29 (1989).

[33] H. X. Gao and L.-M. Peng, Acta Crystallogr., Sect. A: Found. Crystallogr. **55**, 926 (1999).

[34] A. Winkelmann, B. Schröter, and W. Richter, Surf. Sci. **515**, 126 (2002).

[35] B. Schröter, A. Winkelmann, and W. Richter, J. Electron Spectrosc. Relat. Phenom. **114**, 443 (2001).

[36] K. Z. Baba-Kishi, J. Mater. Sci. **37**, 1715 (2002).

[37] R. Fasel, P. Aebi, J. Osterwalder, L. Schlapbach, R. G. Agostino, and G. Chiarello, Phys. Rev. B **50**, 14 516 (1994).

[38] J. R. Michael and J. A. Eades, Ultramicroscopy **81**, 67 (2000).

[39] S. Omori, H. Ishii, and Y. Nihei, Jpn. J. Appl. Phys., Part 2 **36**, L1689 (1997).

[40] S. Omori and Y. Nihei, Jpn. J. Appl. Phys., Part 2 **37**, 4076 (1998).